

ENGINEERING DEPT. LIBRARY
CHANCE VUGHT AIRCRAFT
STRATFORD, CONN.



RESEARCH MEMORANDUM

THIS DOCUMENT AND EACH AND EVERY
PAGE HEREIN IS HEREBY RECLASSIFIED

FROM *Restricted* TO *Unclassified*
AS PER LETTER DATED *Declassification*

PRELIMINARY INVESTIGATION AT LOW SPEEDS OF
Notice # 3
SWEPT WINGS IN ROLLING FLOW

By

David Feigenbaum and Alex Goodman

Langley Memorial Aeronautical Laboratory
Langley Field, Va.

CLASSIFIED DOCUMENT

This document contains classified information affecting the National Defense of the United States within the meaning of the Espionage Act, USC 5031 and its transmission or the revelation of its contents in any manner to an unauthorized person is prohibited by law. Information so classified may be imparted only to persons in the military and naval service of the United States, appropriate civilian officers and employees of the Federal Government who have a legitimate interest therein, and to United States citizens of known loyalty and discretion who of necessity must be informed thereof.

NATIONAL ADVISORY COMMITTEE FOR AERONAUTICS

WASHINGTON

May 22, 1947

RESTRICTED

NATIONAL ADVISORY COMMITTEE FOR AERONAUTICS

RESEARCH MEMORANDUM

PRELIMINARY INVESTIGATION AT LOW SPEEDS OF

SWEPT WINGS IN ROLLING FLOW

By David Feigenbaum and Alex Goodman

SUMMARY

An investigation was conducted to determine the characteristics of a series of untapered wings having angles of sweepback of -45° , 0° , 45° , and 60° under conditions simulating rolling flight. The rolling-flow equipment of the Langley stability tunnel was used to measure all six force and moment components. The characteristics of the wings in straight flow were also determined during the course of the investigation to afford a comparison with previous results. Tests were also conducted to determine the characteristics of ailerons on the 45° sweptback wing in both straight and rolling flow.

In general, the results of tests of the wings in straight flow were consistent with results obtained in previous low-scale investigations.

The tests in rolling flow showed that, for the swept wings, the lateral-force coefficient varied with wing-tip helix angle. Because of this variation, the yawing-moment coefficient at a given rate of roll will be dependent upon the value of the lateral-force coefficient at that rate of roll.

Although the value of the derivative of yawing-moment coefficient with respect to wing-tip helix angle was negative for all positive lift coefficients up to the stall for the unswept wing, the value of this derivative for each of the swept wings changed from negative to positive at some moderate lift coefficient.

In general, the damping in roll became more negative with increasing values of the lift coefficient for all the swept wings tested. Tests on the 45° sweptback wing showed an appreciable reduction in the rate of change of wing-tip helix angle with aileron angle because of the increased damping in roll at the higher lift coefficients.

INTRODUCTION

A knowledge of the rotary stability derivatives is required before calculations can be made to determine the dynamic stability of an airplane or the motions of an airplane after a control displacement. Theoretical values of the derivatives of the forces and moments due to rolling, pitching, or yawing have been used in the past because of the difficulty of obtaining experimental results with conventional test equipment. The calculated values of these derivatives have served fairly well for the determination of the dynamic behavior of unswept or moderately swept wings. Good theoretical values for the stability derivatives of highly swept wings, however, have not yet been obtained, and calculations have failed to predict accurately the dynamic behavior of airplanes with highly swept wings. Several of the rotary derivatives have been determined experimentally for both unswept and swept wings using the forced rotation and oscillation methods described in references 1 and 2. These methods give reliable results for certain derivatives but cannot be conveniently used to determine the derivatives of all six forces and moments with respect to rotation about each of the axes. All of the force and moment derivatives with respect to rolling can be determined rather simply, however, by means of the rolling flow method described in reference 3. The results of reference 3 and unpublished data on swept wings indicate that the value of the rolling moment due to rolling obtained by the rolling flow method are in good agreement with values obtained by the forced rotation method.

The results of a preliminary investigation of a series of untapered swept wings in both straight and rolling flow are presented in this paper.

SYMBOLS

The data are presented in the form of standard NACA coefficients of forces and moments which are referred in all cases to the stability axes, with the origin at the quarter chord point of the mean geometric chord of the models tested. The positive directions of the forces, moments, and angular displacements are shown in figure 1. The coefficients and symbols used herein are defined as follows:

C_L lift coefficient $\left(\frac{L}{qS}\right)$

C_X	longitudinal-force coefficient $\left(\frac{X}{qS}\right)$
C_Y	lateral-force coefficient $\left(\frac{Y}{qS}\right)$
C_l	rolling-moment coefficient $\left(\frac{L'}{qSb}\right)$
C_m	pitching-moment coefficient $\left(\frac{M}{qSc}\right)$
C_n	yawing-moment coefficient $\left(\frac{N}{qSb}\right)$
L	lift, pounds
X	longitudinal force, pounds
Y	lateral force, pounds
L'	rolling moment about X-axis, foot-pounds
M	pitching moment about Y-axis, foot-pounds
N	yawing moment about Z-axis, foot-pounds
q	dynamic pressure, pounds per square foot $\left(\frac{1}{2}\rho V^2\right)$
ρ	mass density of air, slugs per cubic foot
V	free-stream velocity, feet per second
S	wing area, square feet
b	span of wing, measured perpendicular to axis of symmetry, feet
c	chord of wing, measured parallel to axis of symmetry, feet
\bar{c}	mean geometric chord, feet $\left(\frac{2}{S} \int_0^{b/2} c^2 db\right)$
x	distance of quarter-chord point of any chordwise section from the leading edge of the root section, feet

\bar{x} distance from leading edge of root chord to the quarter

chord of the mean geometric chord, feet $\left(\frac{2}{S} \int_0^{b/2} cx \, db \right)$

A aspect ratio $\left(\frac{b^2}{S} \right)$

α angle of attack measured in plane of symmetry, degrees

Λ angle of sweep positive for sweepback, degrees

ψ angle of yaw, degrees

$\frac{pb}{2V}$ wing-tip helix angle, radians

δ_a aileron deflection measured in plane perpendicular to aileron hinge axis, degrees

$$C_{L\alpha} = \frac{\partial C_L}{\partial \alpha}$$

$$C_{Y\psi} = \frac{\partial C_Y}{\partial \psi}$$

$$C_{Yp} = \frac{\partial C_Y}{\partial \left(\frac{pb}{2V} \right)}$$

$$C_{l\psi} = \frac{\partial C_l}{\partial \psi}$$

$$C_{lp} = \frac{\partial C_l}{\partial \left(\frac{pb}{2V} \right)}$$

$$C_{n\psi} = \frac{\partial C_n}{\partial \psi}$$

$$C_{np} = \frac{\partial C_n}{\partial \left(\frac{pb}{2V} \right)}$$

APPARATUS AND TESTS

The tests of the present investigation were conducted in the 6-foot circular test section of the Langley stability tunnel which is equipped with a motor-driven rotor and vanes for rotating the air stream about the tunnel axis (see reference 3). The models were rigidly mounted at the quarter-chord of the mean geometric chord on a single strut support (fig. 2) which was attached to a conventional six-component balance. By means of this equipment, rolling flight is simulated by rolling the air stream with respect to the rigidly mounted model.

The models tested consisted of four untapered wings of approximately the same area, all of which had equal chords (10 in.) and NACA 0012 sections in planes normal to the leading edge (see fig. 3). The wings had sweepback angles of -45° , 0° , 45° , and 60° and the corresponding aspect ratios were 2.61, 5.16, 2.61, and 1.34, respectively. The 45° sweptback wing was equipped with 20-percent wing chord and 50-percent wing semispan plain ailerons. The aileron nose gaps were sealed with plasticine.

All tests were run at a dynamic pressure of 39.7 pounds per square foot, which corresponds to a Mach number of 0.17. The test Reynolds numbers, based on the mean geometric chords of the models, are

Sweepback (deg)	Reynolds number
-45	1,400,000
0	990,000
45	1,400,000
60	1,980,000

The characteristics of these wings were determined in both straight and rolling flow. In the straight flow tests, six-component measurements were obtained for each wing through an angle-of-attack range from approximately zero lift up to and beyond maximum lift at angles of yaw of 0° and $\pm 5^\circ$. Tests were also made at angles of attack of approximately 0° , 6° , and 12° through a yaw-angle range of from -30° to 30° .

The rolling flow tests were made at positive and negative rotor speeds corresponding to a constant value of wing-tip helix angle $\frac{pb}{2V}$ of 0.0446 through the same angle-of-attack range used for the straight flow tests. Tests were also made at angles of attack of approximately 0° , 6° , and 12° through a range of positive and negative rotor speeds.

Both straight-flow and rolling-flow characteristics of the 45° sweptback wing with ailerons $(0.20c, 0.50\frac{b}{2})$ were obtained for angles of attack of approximately 0° , 6° , and 12° and for aileron deflections of $\pm 10^\circ$, $\pm 15^\circ$, and $\pm 30^\circ$.

CORRECTIONS

Although there has been no systematic investigation of tunnel corrections for swept wings, calculations for a few specific models have indicated that corrections for tunnel wall effect are determined primarily by the spans and areas of models and are not greatly affected by sweep. Corrections previously developed for unswept wings therefore were applied to the present wings regardless of the angle of sweep. The corrections were made to longitudinal-force coefficients, rolling-moment coefficients, and angles of attack by the following equations:

$$\Delta C_X = \delta_w \left(\frac{S}{C} \right) C_L^2$$

$$\Delta C_{l_t} = K C_{l_t}$$

$$\Delta \alpha = 57.3 \delta_w \left(\frac{S}{C} \right) C_L$$

where

δ_w boundary correction factor obtained from reference 4

C tunnel cross-section area, square feet

C_{l_t} uncorrected rolling-moment coefficient

K a correction factor from reference 5 modified for application to these tests

The data have not been corrected for the effects of blocking or for the support strut tares. Several tare measurements were made and they indicated that, in general, the corrections would be very small.

RESULTS AND DISCUSSION

Presentation of Data

The data obtained in the straight flow tests are presented in figures 4 to 8. The results of the tests made through the angle-of-attack range for $\pm 5^\circ$ yaw are not presented because they were used only for determining the lateral stability derivatives which are presented in figures 9 and 10.

The data obtained in the rolling-flow tests are presented in figures 11 to 14. The results of the tests made through the angle-of-attack range at values of $\frac{pb}{2V}$ of ± 0.0446 are not presented because they were used only to determine the rotary stability derivatives which are presented in figures 15 and 16.

The characteristics obtained from the ailerons tested on the 45° sweptback wing in both straight and rolling flow are presented in figure 17.

Characteristics in Straight Flow

The characteristics of the present series of swept wings obtained in straight flow are approximately the same as would be expected on the basis of previous low-scale tests. (See reference 6.) The aspect ratios of the swept wings used in the present investigation differed from those reported in reference 6. The wings of the present series all had approximately the same area and the aspect ratio reduced with sweep angle approximately as the $\cos^2 \Lambda$. Because of the variation between aspect ratio and sweep angle, the relations for $C_{L\alpha}$

and $\frac{\partial C_N}{\partial C_L}$ as given in reference 6 reduce to

$$C_{L\alpha} = \left(C_{L\alpha} \right)_{\Lambda=0} \cos \Lambda$$

IF DATA CORRECTED FOR
AR IN ROLLING FLOW
RELATIONS WOULD BE

$$C_{L\alpha} = (C_{L\alpha})_{AR=1} (\cos^2 \Lambda)^{0.67}$$

BAC 7-15

$$\frac{\partial C_{L\psi}}{\partial C_L} = \left(\frac{\partial C_{L\psi}}{\partial C_L} \right)_{\Lambda=0} + \frac{1}{4} \frac{\tan \Lambda}{57.3}$$

A comparison of the calculated and experimental values for these derivatives is shown in figure 10. The agreement is reasonably good although the calculated values underestimate the effects of sweep.

It should be noted that the values for the 45° sweptforward wing deviate from the calculated values slightly more than do the values for the 45° sweptback wing. Also noticeable about the 45° sweptforward wing (see fig. 4) is that its aerodynamic center is located farther back on the mean geometric chord (0.32 mean geometric chord) than the aerodynamic centers of the unswept or sweptback wings (0.19 to 0.22 mean geometric chord) and that its maximum lift coefficient (about 0.8) is lower than that of the unswept or 45° sweptback wings (about 1.0) and much lower than that of the 60° sweptback wing (about 1.2 at $\alpha = 36^\circ$). The value of $C_{L\psi}$ for the 45° sweptforward wing is practically zero up to a lift coefficient of about 0.6 (see fig. 9), and the maximum positive value of $C_{L\psi}$ for the 45° sweptforward wing is about two-thirds the maximum positive value attained by the 45° sweptback wing.

All the wings tested become increasingly stable longitudinally as they approached and exceeded maximum lift coefficient, which is in agreement with the correlation presented in reference 7.

Characteristics in Rolling Flow

The data presented in figures 11 to 14 indicate that for angles of attack up to a least 12° , the values C_L , C_X , and C_m are practically unaffected by the variations in $\frac{pb}{2V}$ within the range investigated, and that C_Y , C_l , and C_n vary linearly with $\frac{pb}{2V}$. Unpublished data on tests of the 45° sweptback wing show that this linear variation of C_l and C_n with $\frac{pb}{2V}$ holds even beyond the stall, at least for a range of $\frac{pb}{2V}$ of ± 0.1 . Because of this linearity the

method of obtaining the derivatives C_{Y_p} , C_{l_p} , and C_{n_p} from the differences in the coefficients for just two values of wing-tip helix angle was considered applicable through the complete angle-of-attack range used for the present tests. The derivatives obtained from tests at values of $\frac{pb}{2V}$ of ± 0.0446 are presented in figure 15.

Dynamic stability calculations in the past have neglected the effects of variation of lateral force with rate of roll since such a variation was not found to exist for unswept wings below the stall. For swept wings, however, such a variation does exist as indicated in figure 15. Figure 15 shows that for a limited range the values of C_{Y_p} are nearly proportional to the lift coefficient, which would be expected from calculations based on the simplified theory discussed in reference 6. At moderate lift coefficients, however, the values of C_{Y_p} for the swept wings markedly decreased in magnitude, in some cases even reversing sign.

For the unswept wing, the negative value of C_{n_p} varied linearly with lift coefficient up to the maximum lift coefficient. The values of C_{n_p} for the swept wings, however, were proportional to the lift coefficient for only a limited range and, at moderate lift coefficients, reversed sign and assumed large positive values. For low lift coefficients the values of the slope $\left(\frac{\partial C_{n_p}}{\partial C_L} \right)_{C_L=0}$ (see fig. 16) became more negative as the angle of sweepback was increased.

The values of C_{n_p} shown in figure 15 are for moments taken about the quarter-chord point of the mean geometric chord shown in figure 3. Because of the existence of the derivative C_{Y_p} for swept wings, the value of C_{n_p} will vary with the longitudinal location of the point about which the moments are calculated. That these two derivatives are interdependent is indicated in figure 15 by the fact that both undergo abrupt variations in slope at the same lift coefficients.

For the unswept wing, the value of the damping in roll C_{l_p} was nearly independent of lift coefficient up to the maximum lift

coefficient, beyond which the sign of C_{l_p} changed from negative to positive. The values of C_{l_p} for the swept wings generally become more negative with an increasing value of lift coefficient over the greater part of the lift-coefficient range. No positive values of C_{l_p} were obtained for the swept wings for the range of angle of attack tested, even beyond the maximum lift coefficient.

Application of the simplified theory to the present series of wings leads to the following expression:

$$C_{l_p} = (C_{l_p})_{\Lambda=0} \cos \Lambda$$

A comparison of the calculated values with those measured at low lift coefficients is presented in figure 16 and indicates that the decrease in C_{l_p} with angle of sweep is slightly more rapid than predicted by the calculations.

Aileron Characteristics

The results of the tests made to determine the characteristics of the ailerons on the 45° sweptback wing are presented in figure 17. Tests were made in both straight and rolling flow with both ailerons deflected through the same angle, but in opposite directions. The rolling flow data are for the condition of zero rolling moment. The data indicate that the variation of rolling moment with aileron deflection falls off slightly with increasing angle of attack, which, coupled with the increase of damping in roll with angle of attack, causes the variation in $\frac{pb}{2V}$ with aileron deflection to fall off somewhat rapidly with angle of attack.

For the range of angle of attack considered, the yawing moment due to roll (fig. 15) is of the same sign as the yawing moment due to aileron deflection, (fig. 17(a)) and therefore, the yawing moment of the rolling wing will be greater than that due to the ailerons alone. The lateral force due to roll is of the opposite sign and of a greater magnitude than the lateral force due to aileron deflection, which will result in a reversal of lateral force during the transition

from straight to rolling flight, and positive values of lateral force for the wing in steady roll.

CONCLUSIONS

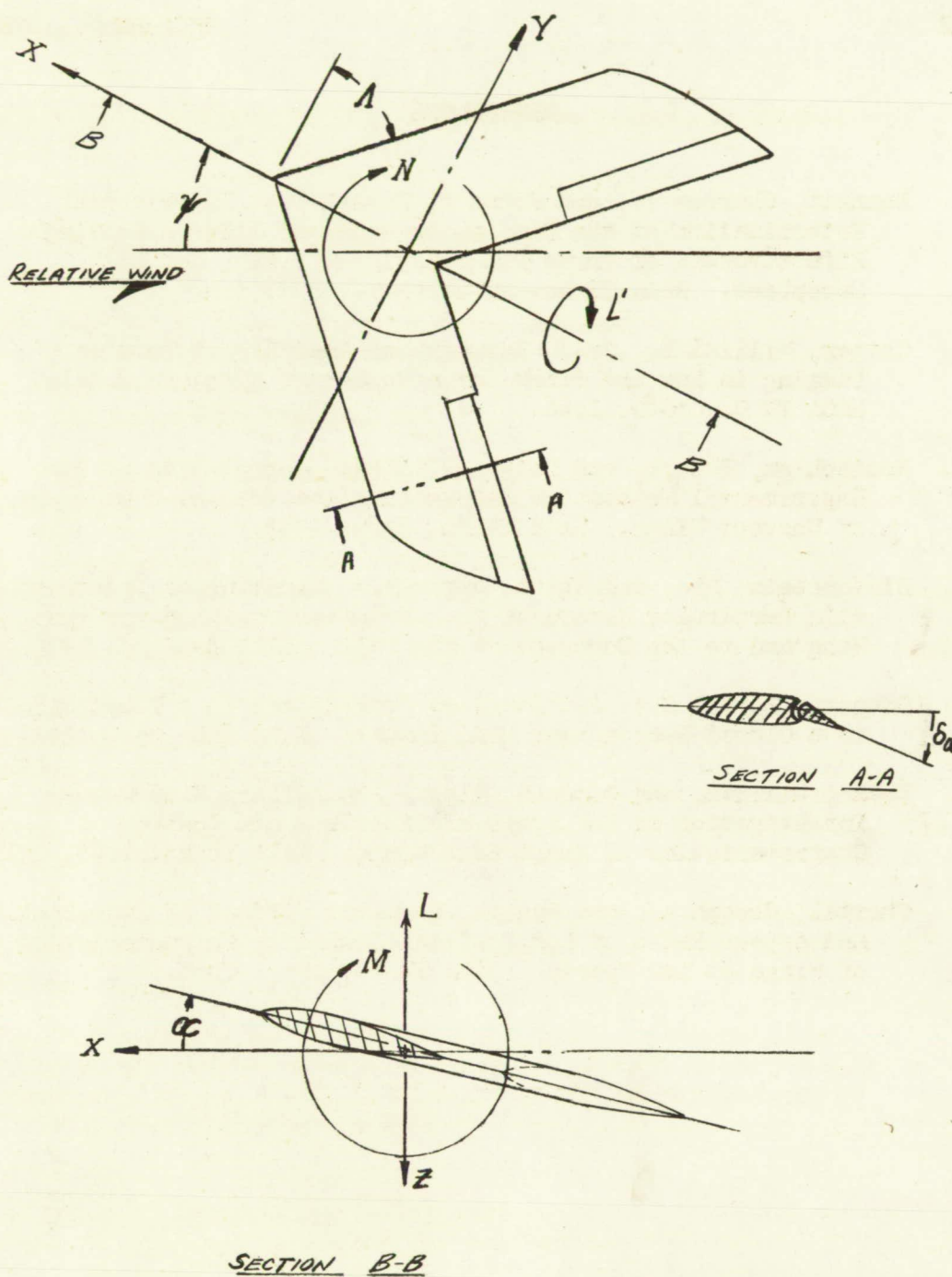
The results of low-scale tests made in straight and rolling flow on a series of untapered swept wings having equal chords in planes normal to the leading edge and approximately equal areas indicate the following conclusions:

1. In general, the characteristics of the wings in straight flow are consistent with results obtained in previous investigations.
2. A variation of lateral-force coefficient with wing-tip helix angle was found to exist for the swept wings. Because of this variation, the yawing-moment coefficient at a given rate of roll will be dependent upon the value of the lateral-force coefficient at that rate of roll.
3. Although the value of the derivative of yawing-moment coefficient with respect to wing-tip helix angle was negative for all positive lift coefficients up to the stall for the unswept wing, the value of this derivative for the swept wings changed from negative to positive at some moderate lift coefficients.
4. The damping in roll generally becomes more negative with increasing values of the lift coefficient for all of the swept wings tested.
5. Tests on the 45° sweptback wing showed an appreciable reduction in the rate of change of helix angle with aileron angle with increasing angle of attack because of the increased damping in roll at higher lift coefficients.

Langley Memorial Aeronautical Laboratory
National Advisory Committee for Aeronautics
Langley Field, Va.

REFERENCES

- ✓1. Bennett, Charles V., and Johnson, Joseph L.: Experimental Determination of the Damping in Roll and Aileron Rolling Effectiveness of Three Wings Having 2° , 42° , and 62° Sweepback. NACA TN No. 1278, 1947.
2. Cotter, William E., Jr.: Summary and Analysis of Data on Damping in Yaw and Pitch for a Number of Airplane Models. NACA TN No. 1080, 1946.
3. MacLachlan, Robert, and Letko, William: Correlation of Two Experimental Methods of Determining the Rolling Characteristics of Unswept Wings. NACA TN No. 1309, 1947.
4. Silverstein, Abe, and White, James A.: Wind-Tunnel Interference with Particular Reference to Off-Center Positions of the Wing and to the Downwash at the Tail. NACA Rep. No. 547, 1935.
5. Swanson, Robert S.: Jet-Boundary Corrections to a Yawed Model in a Closed Rectangular Wind Tunnel. NACA ARR, Feb. 1943.
- ✓6. Letko, William, and Goodman, Alex: Preliminary Wind-Tunnel Investigation at Low Speed of Stability and Control Characteristics of Swept-Back Wings. NACA TN No. 1046, 1946.
7. Shortal, Joseph A., and Maggin, Bernard: Effect of Sweepback and Aspect Ratio on Longitudinal Stability Characteristics of Wings at Low Speeds. NACA TN No. 1093, 1946.



NATIONAL ADVISORY
COMMITTEE FOR AERONAUTICS

Figure 1.- System of axes used. Positive values of forces, moments, and angles are indicated.

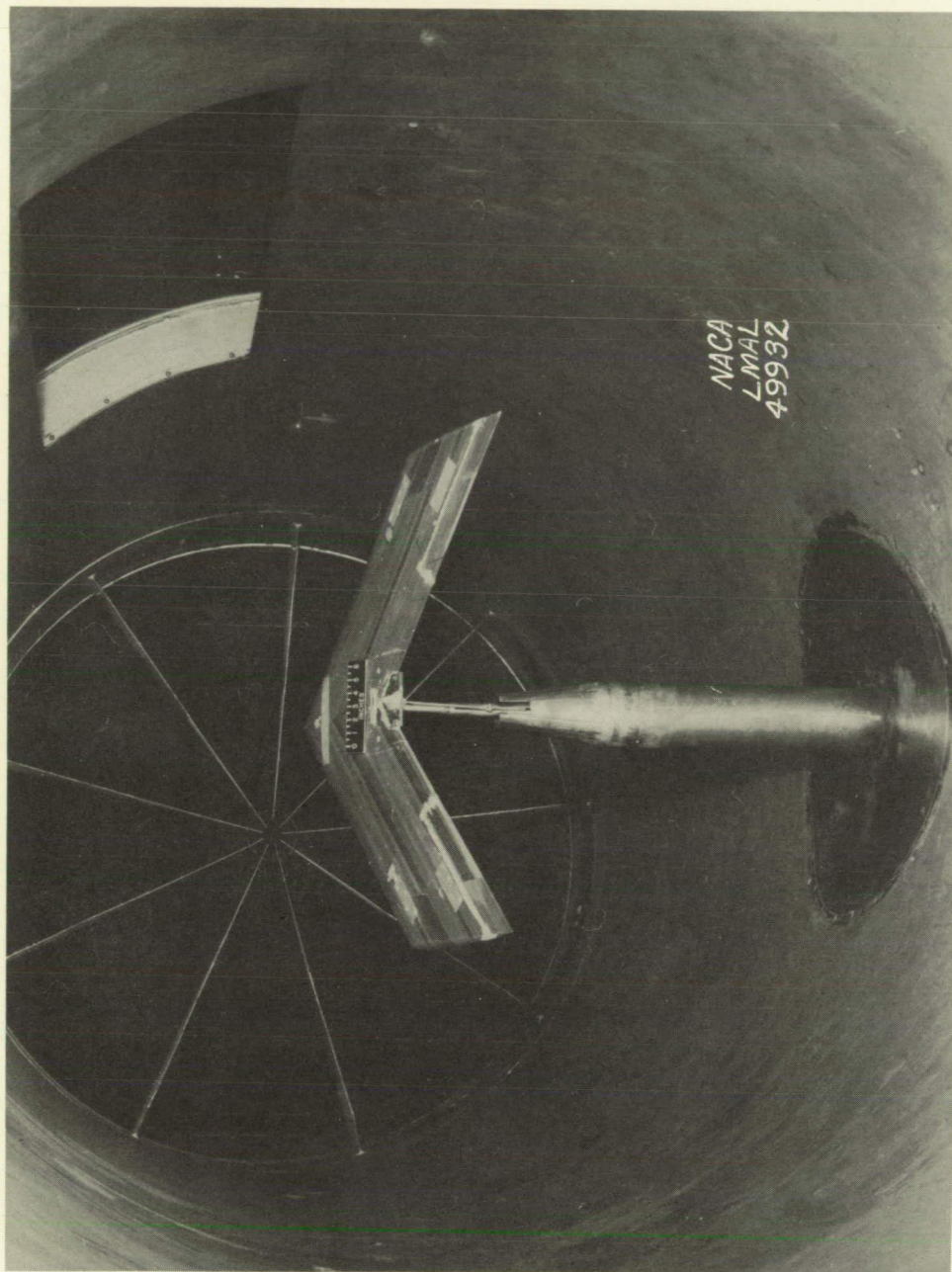
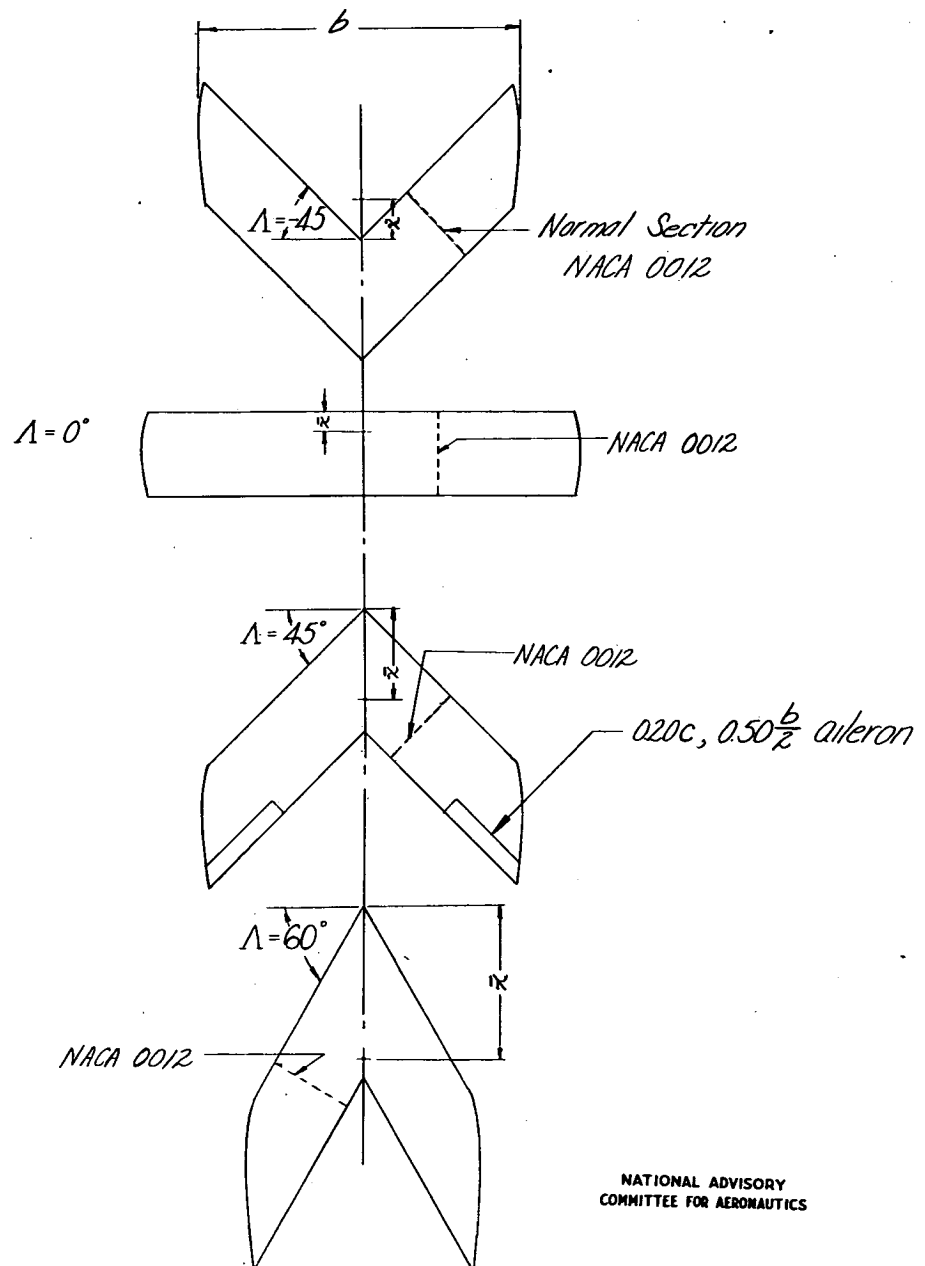


Figure 2.- 45° swept-back wing mounted on the single-strut support in the Langley stability tunnel (rolling-flow test section).

Λ (deg)	A	S (ft. ²)	b (ft.)	\bar{x} (ft.)
-45	2.61	3.56	3.05	-0.460
0	5.16	3.52	4.26	0.208
45	2.61	3.56	3.05	1.050
60	1.34	3.64	2.21	1.360



NATIONAL ADVISORY
COMMITTEE FOR AERONAUTICS

Figure 3.- Planforms of the swept wings tested.

Fig. 4

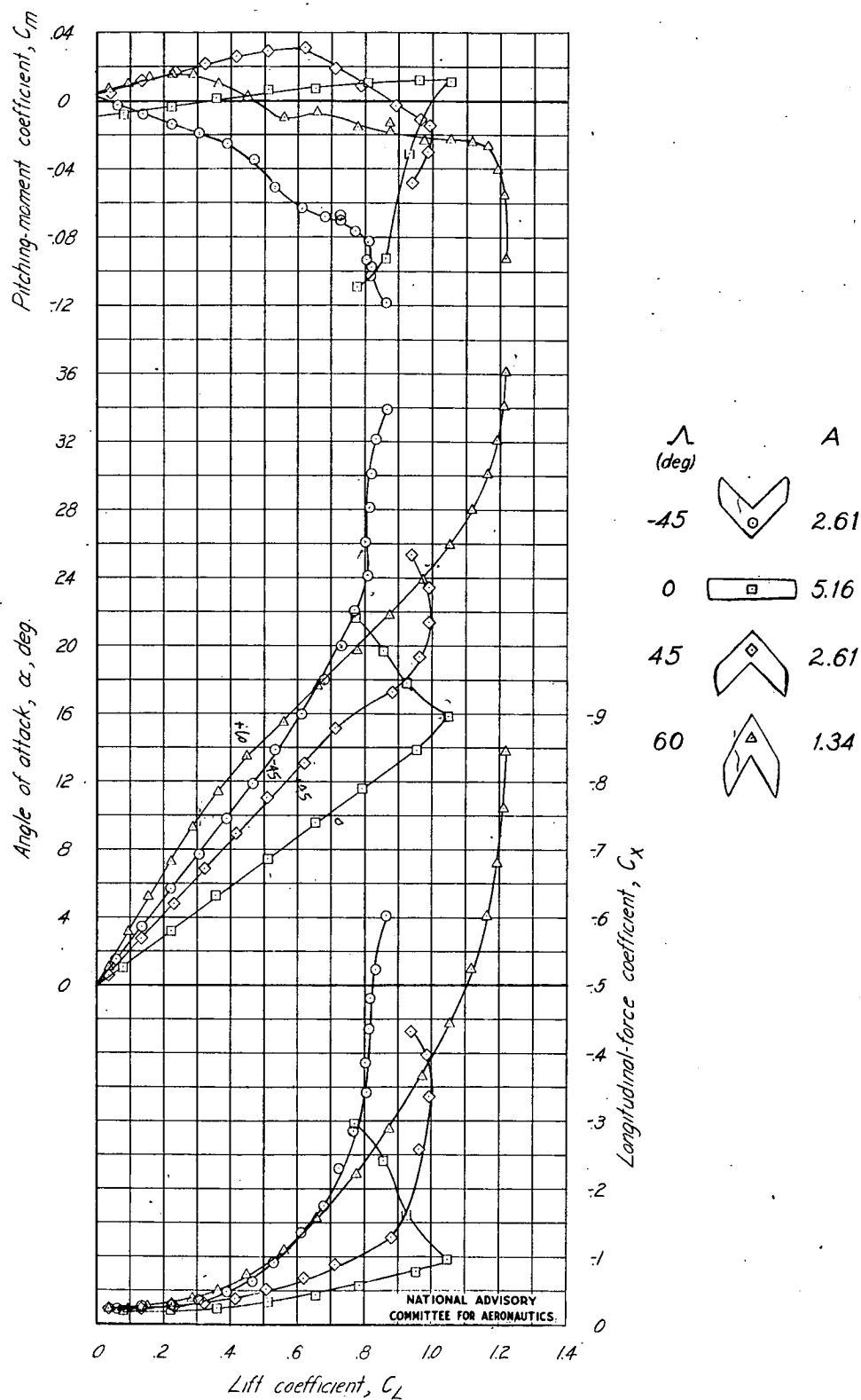


Figure 4.- Variation with lift coefficient of the aerodynamic characteristics of several swept wings.

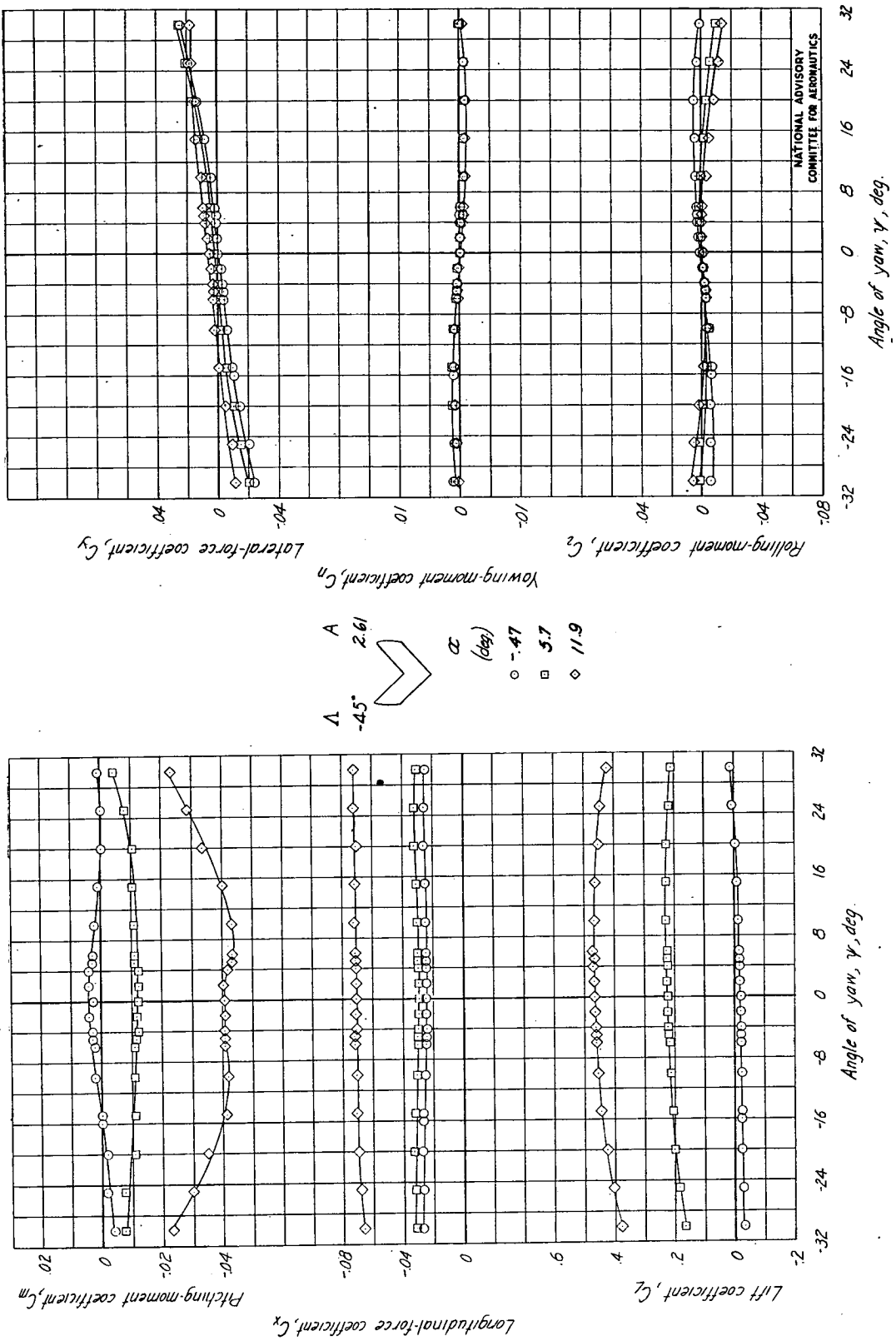


Figure 5.- Variation with angle of yaw of the aerodynamic characteristics of a rectangular 45° swept-forward wing.

Fig. 6

NACA RM No. L7E09

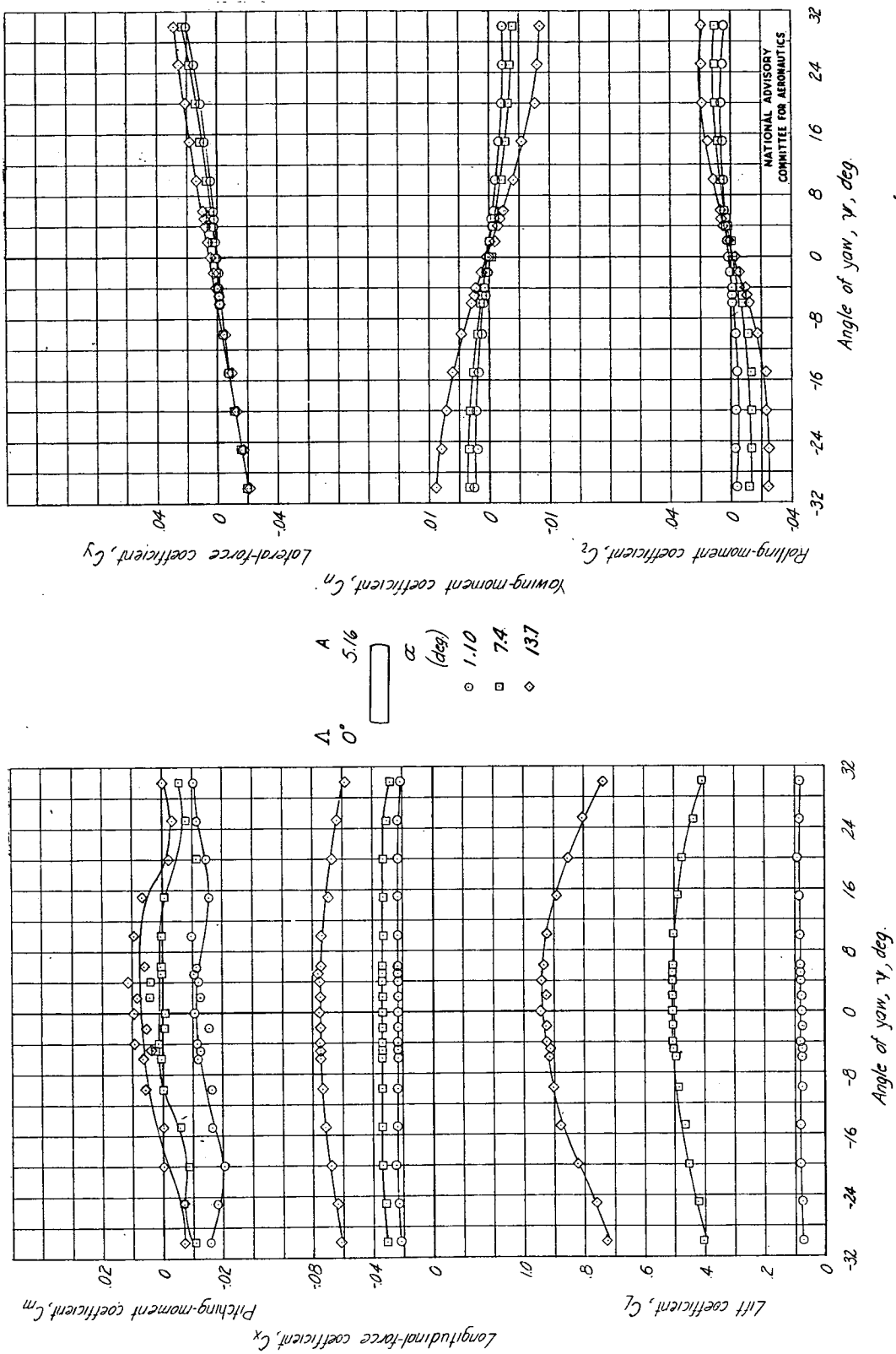


Figure 6- Variation with angle of yaw of the aerodynamic characteristics of a rectangular 0° swept wing.

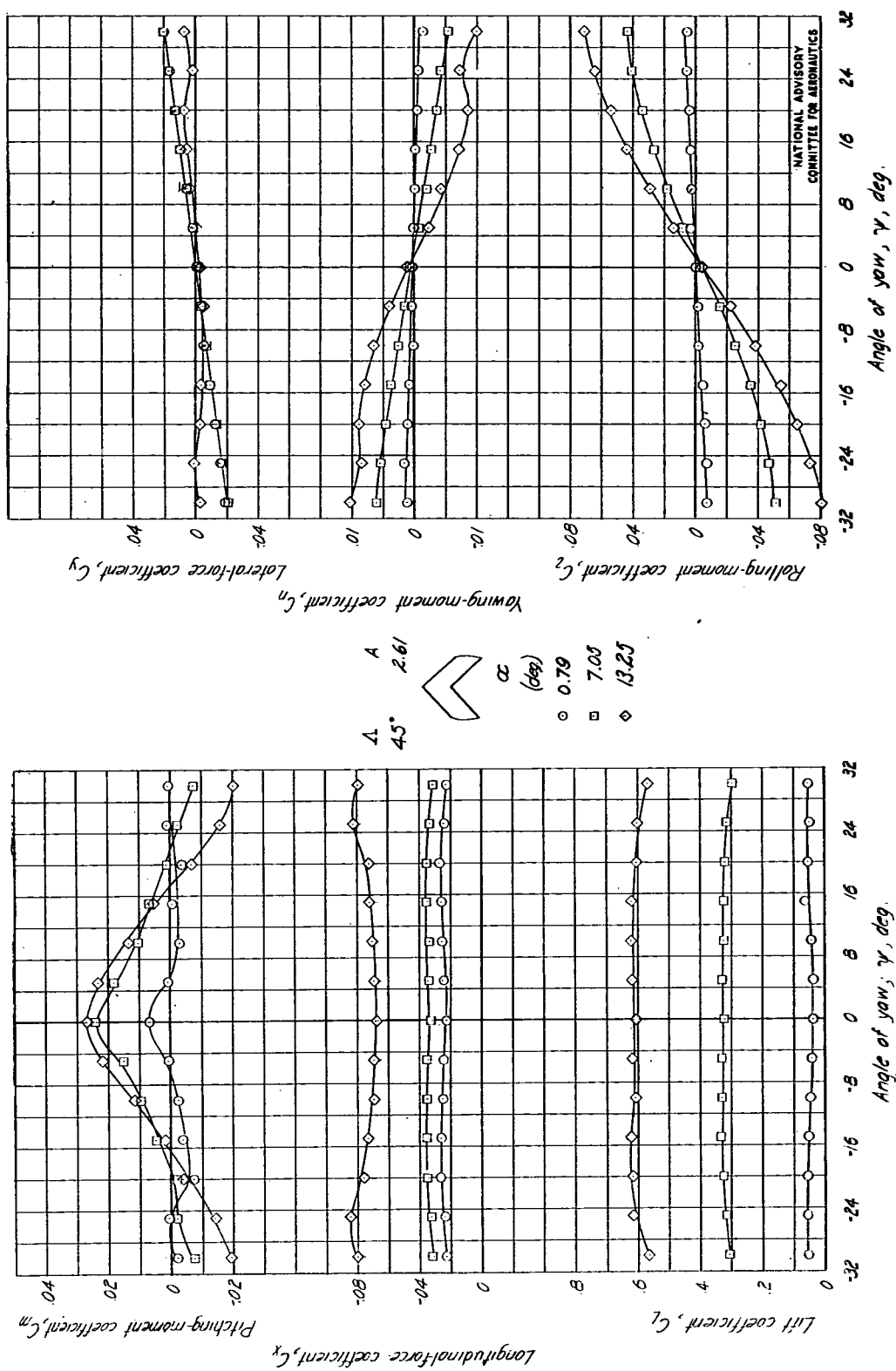


Figure 7- Variation with angle of yaw of the aerodynamic characteristics of a rectangular 45° swept-back wing

Fig. 8

NACA RM No. L7E09

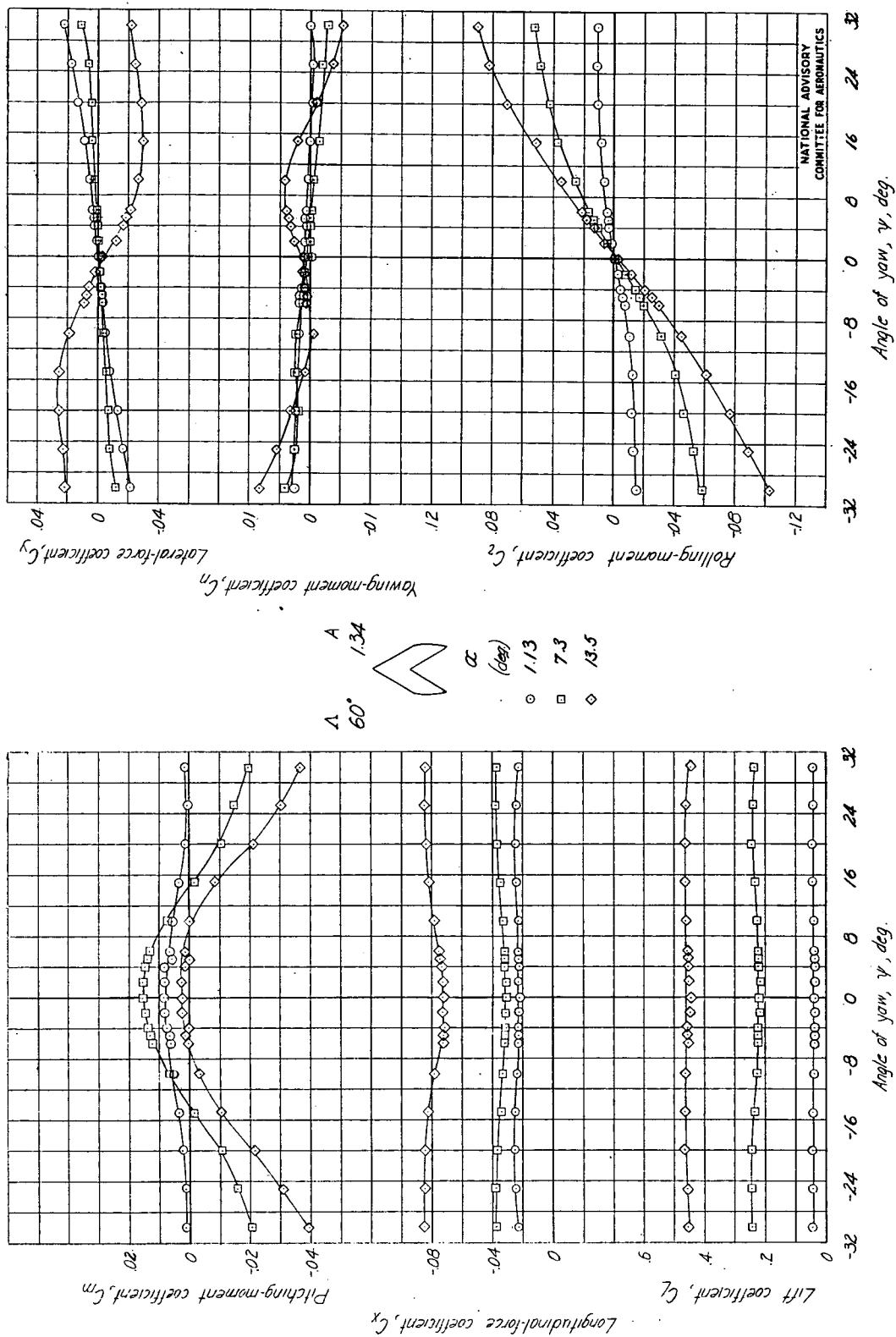


Figure 8.-Variation with angle of yaw of the aerodynamic characteristics of a rectangular 60° swept-back wing.

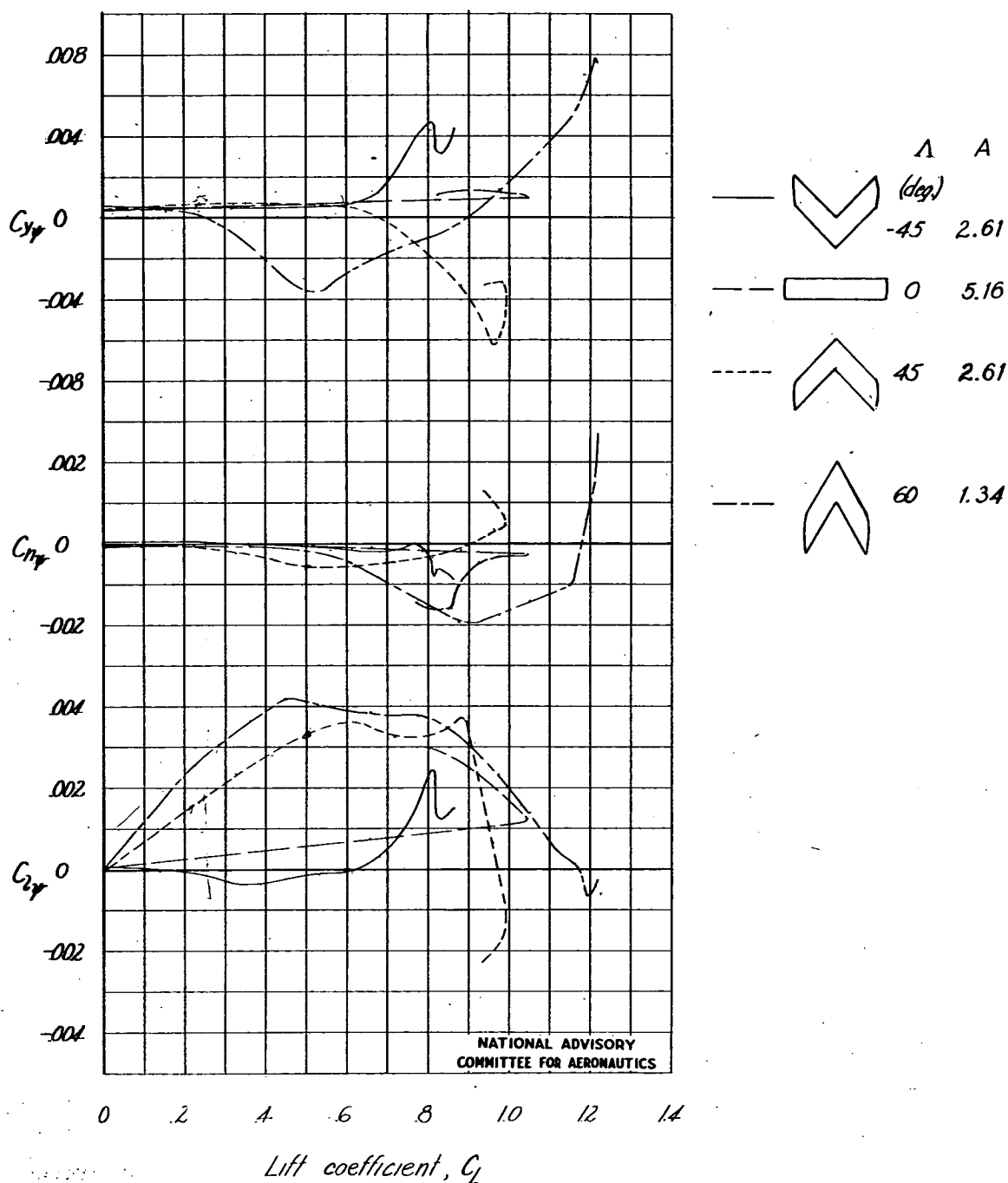


Figure 9.-Variation of $C_{y\psi}$, $C_{n\psi}$, and $C_{z\psi}$ with lift coefficient.

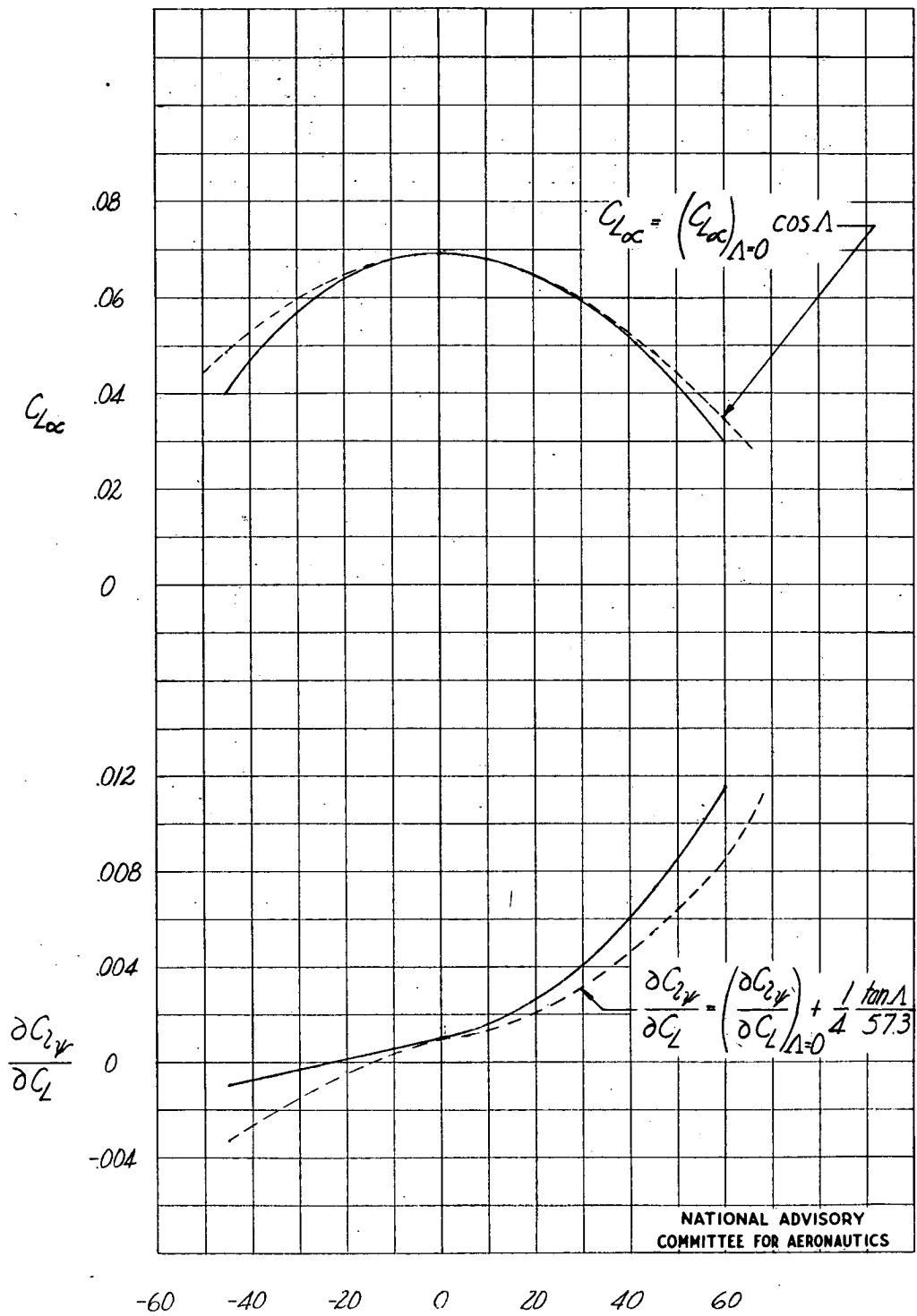


Figure 10.- Variation of the estimated and experimental values of $C_{L\alpha}$ and $\frac{\partial C_{L\alpha}}{\partial C_L}$ with angle of sweep.

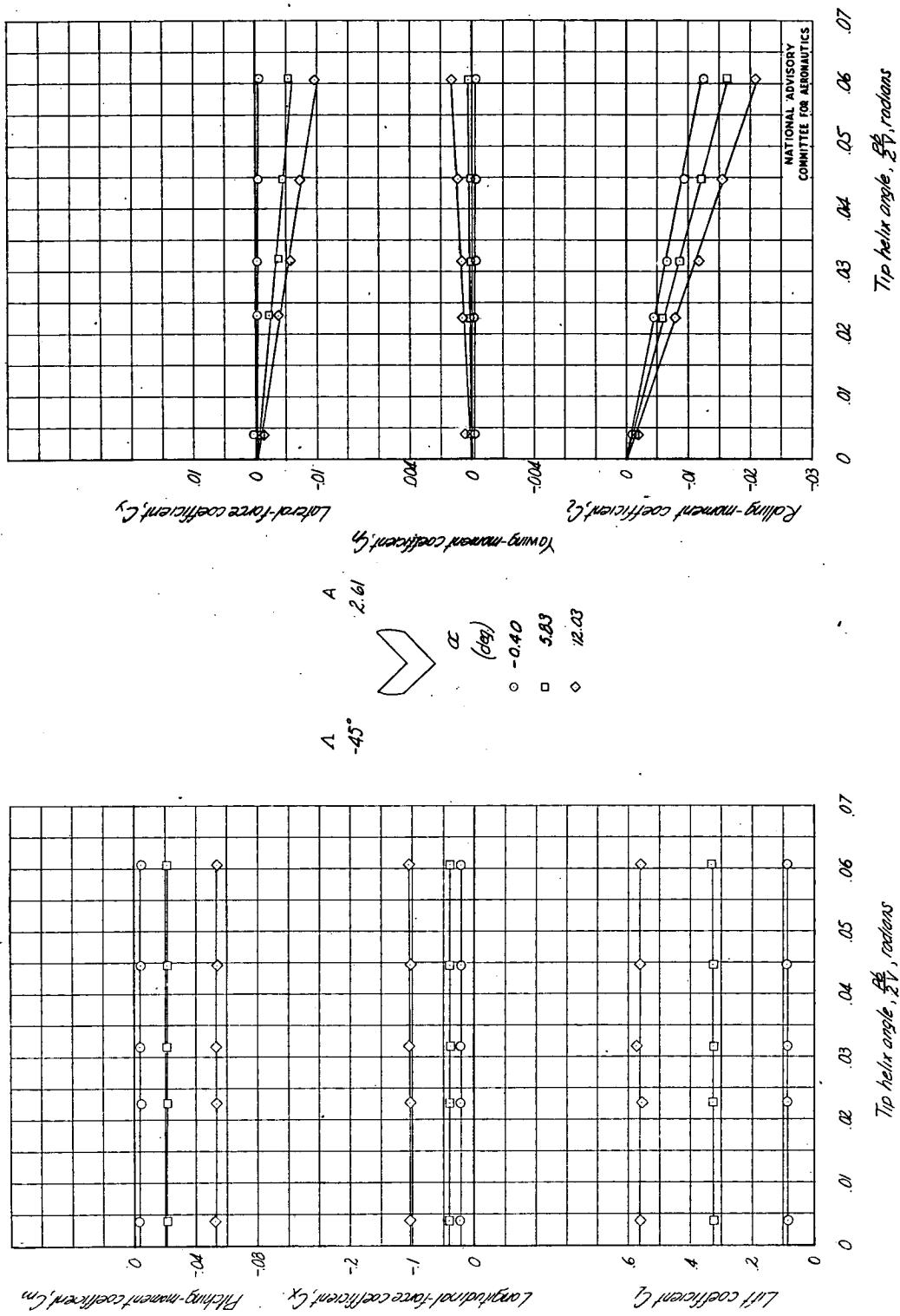


Figure 11. - Variation with tip helix angle of the aerodynamic characteristics of a rectangular 45° swept-forward wing.

Fig. 12

NACA RM No. L7E09

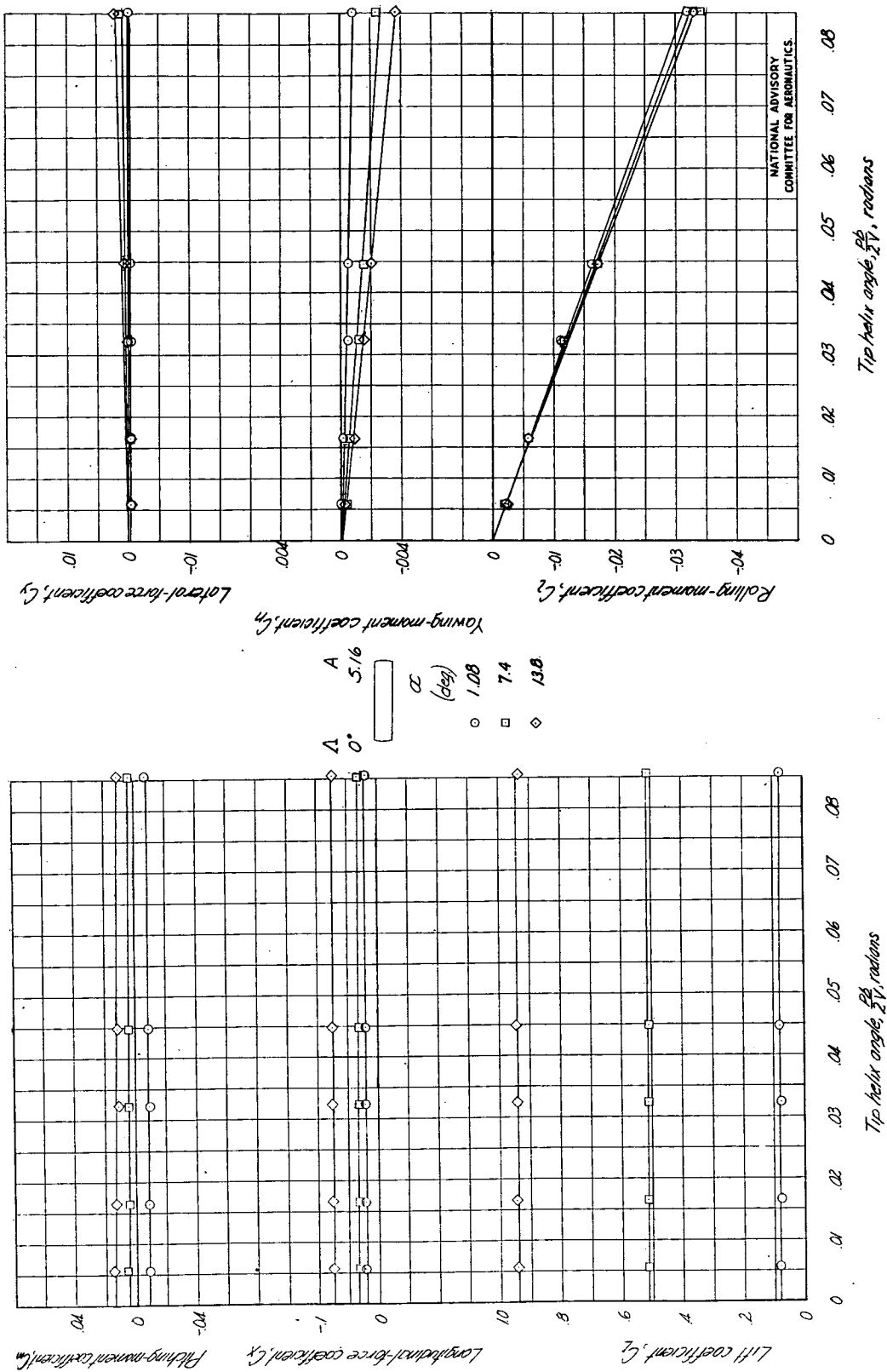


Figure 12-Variation with tip helix angle of the aerodynamic characteristics of a rectangular 0° swept wing.

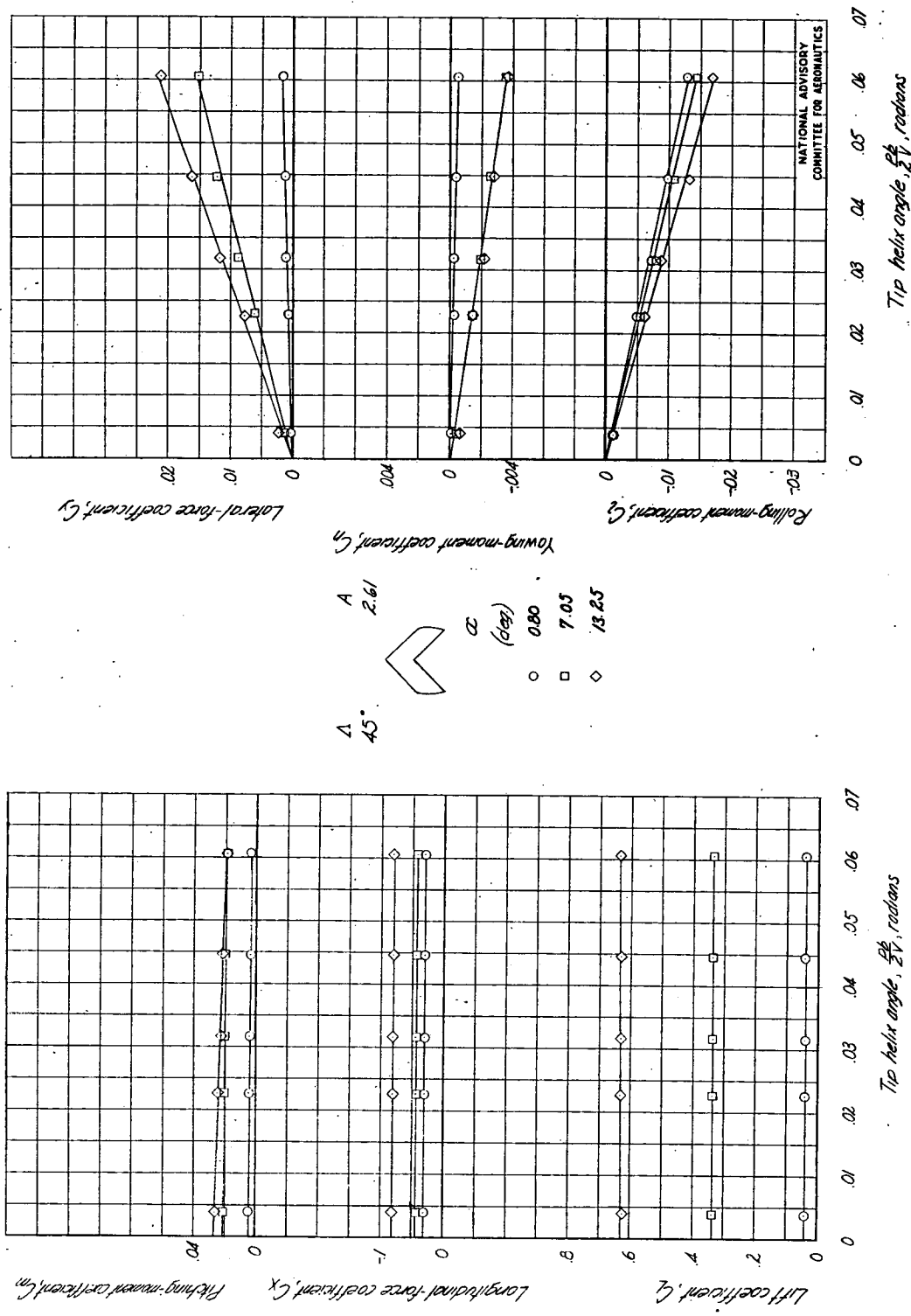


Figure 13- Variation with tip helix angle of the aerodynamic characteristics of a rectangular 45° swept-back wing.

Fig. 14

NACA RM No. L7E09

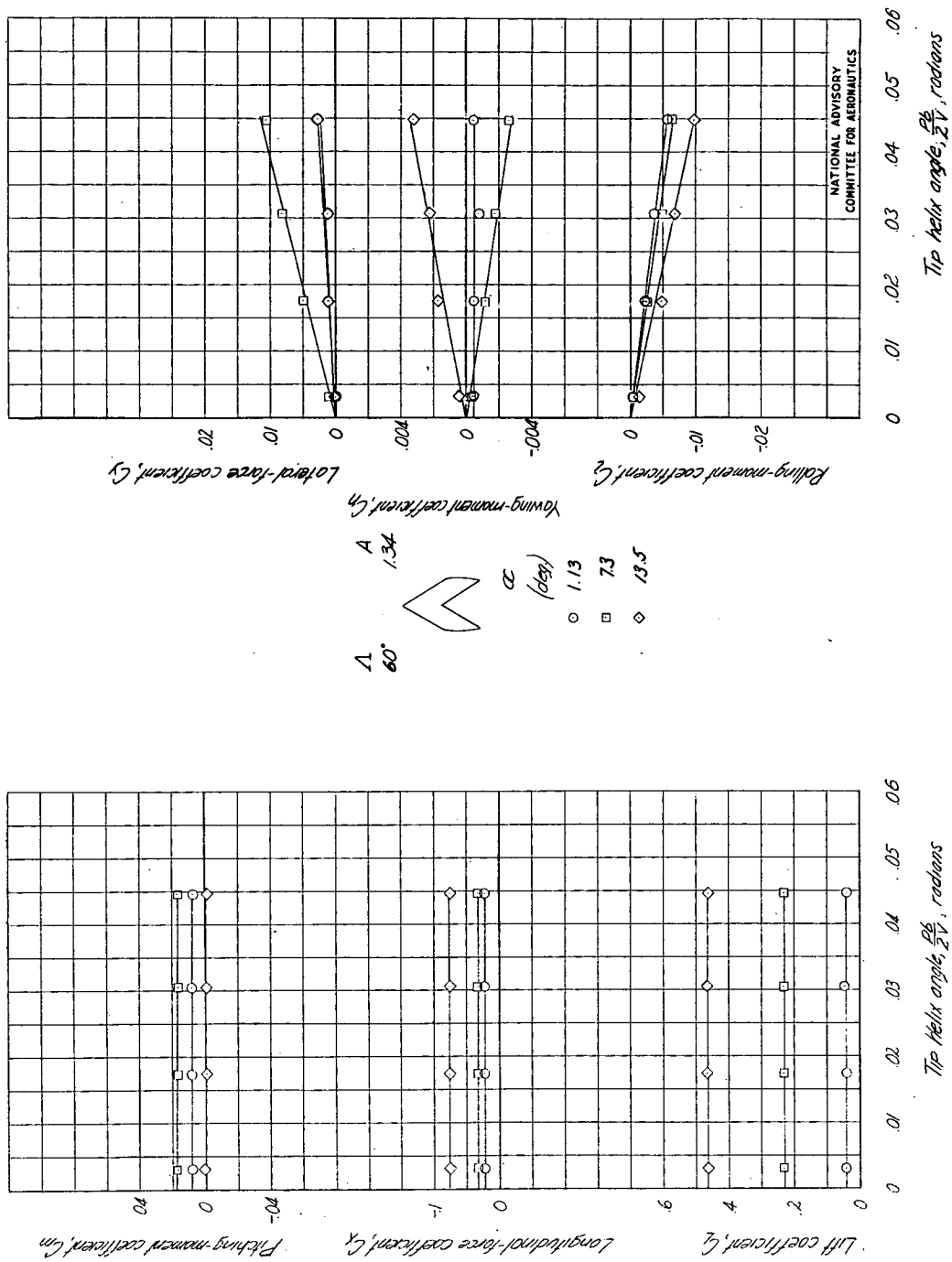


Figure 14- Variation with tip helix angle of the aerodynamic characteristics of a rectangular 60° swept-back wing

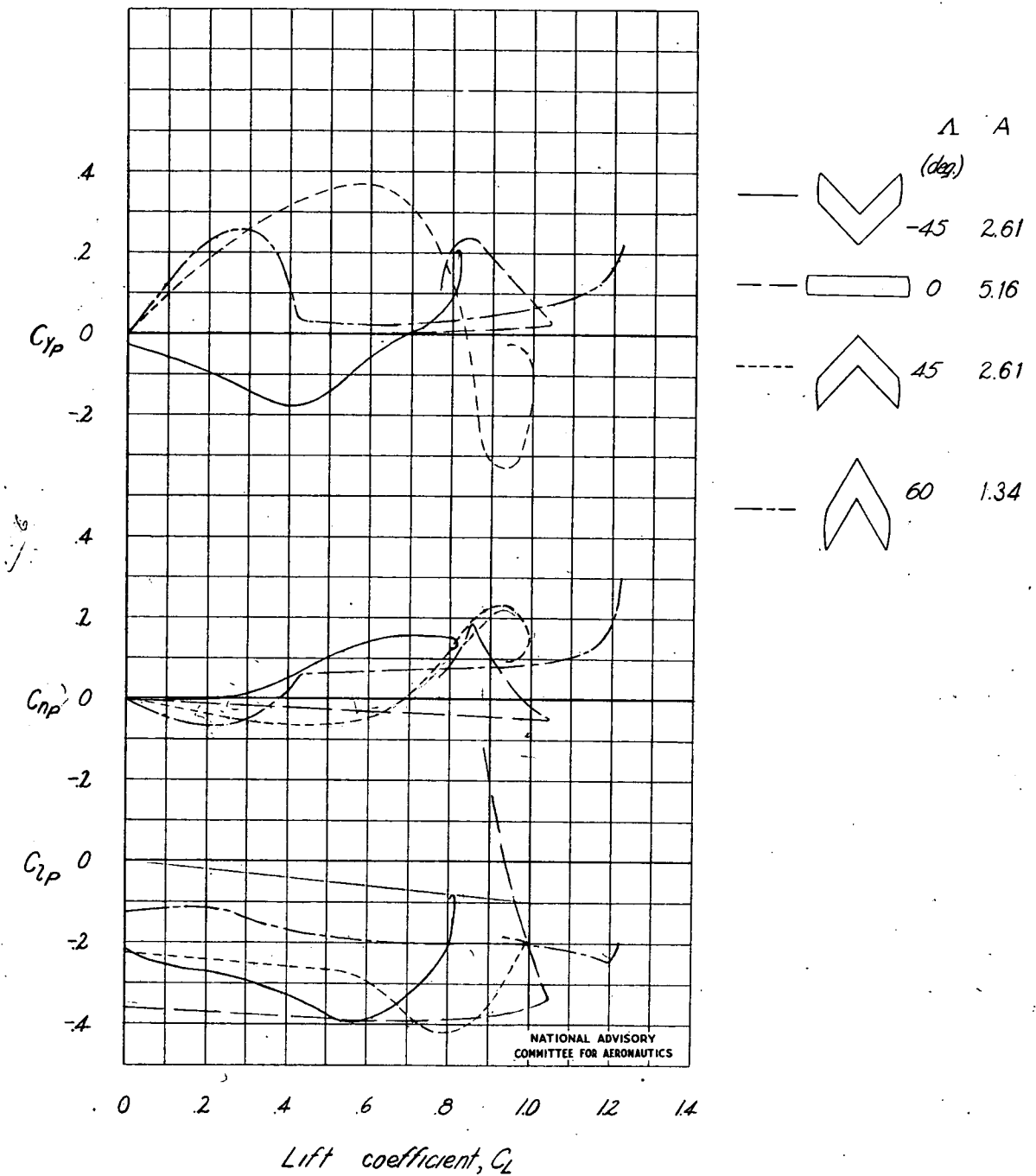
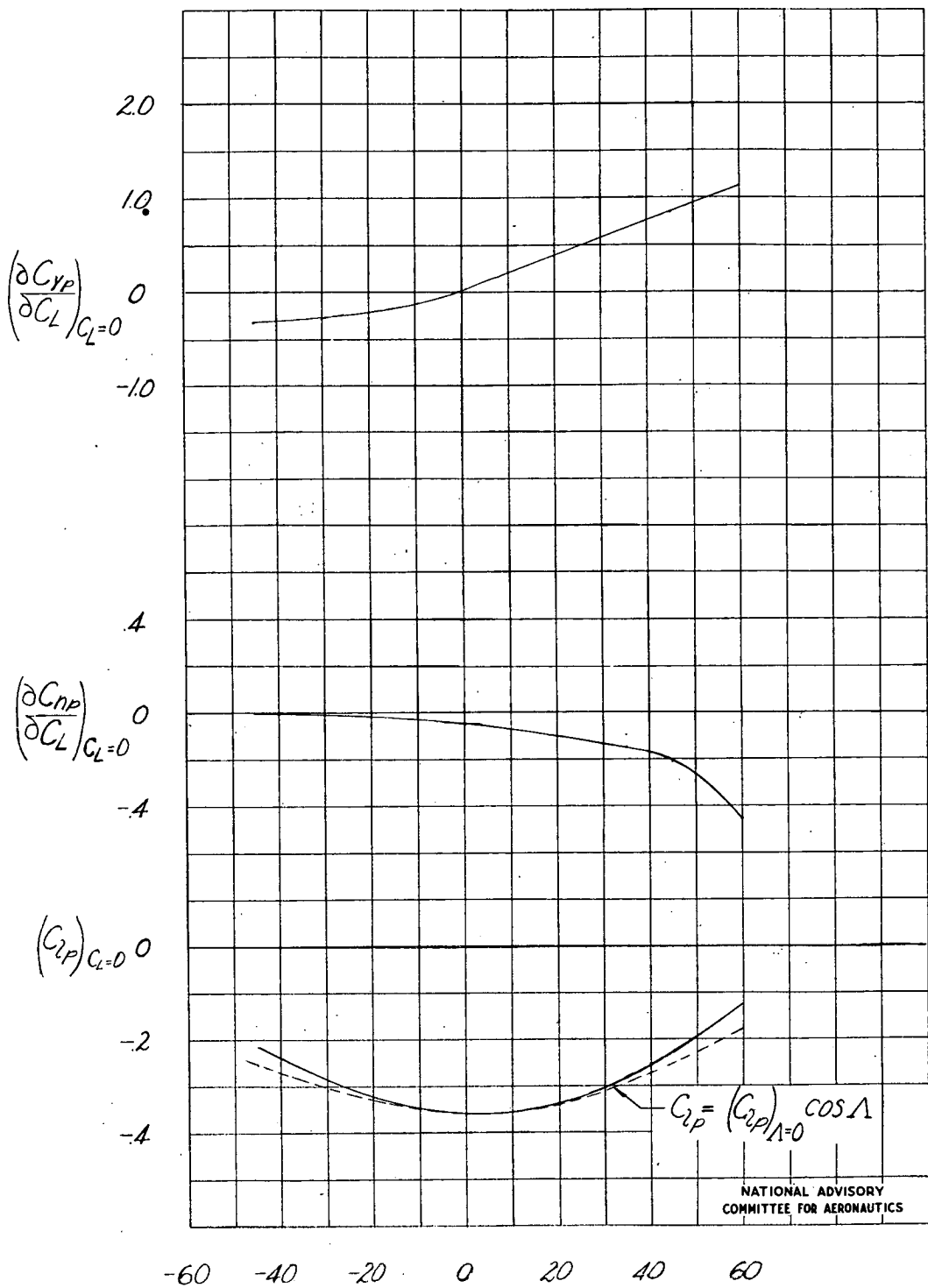


Figure 15.-Variation of C_{yp} , C_{np} , and C_{zp} with lift coefficient.



Angle of sweep, Λ , deg.

Figure 16: Variation of the estimated and experimental values of $\frac{\partial C_{Yp}}{\partial C_L}$, $\frac{\partial C_{np}}{\partial C_L}$, and $(C_L)_{C_L=0}$ with angle of sweep.

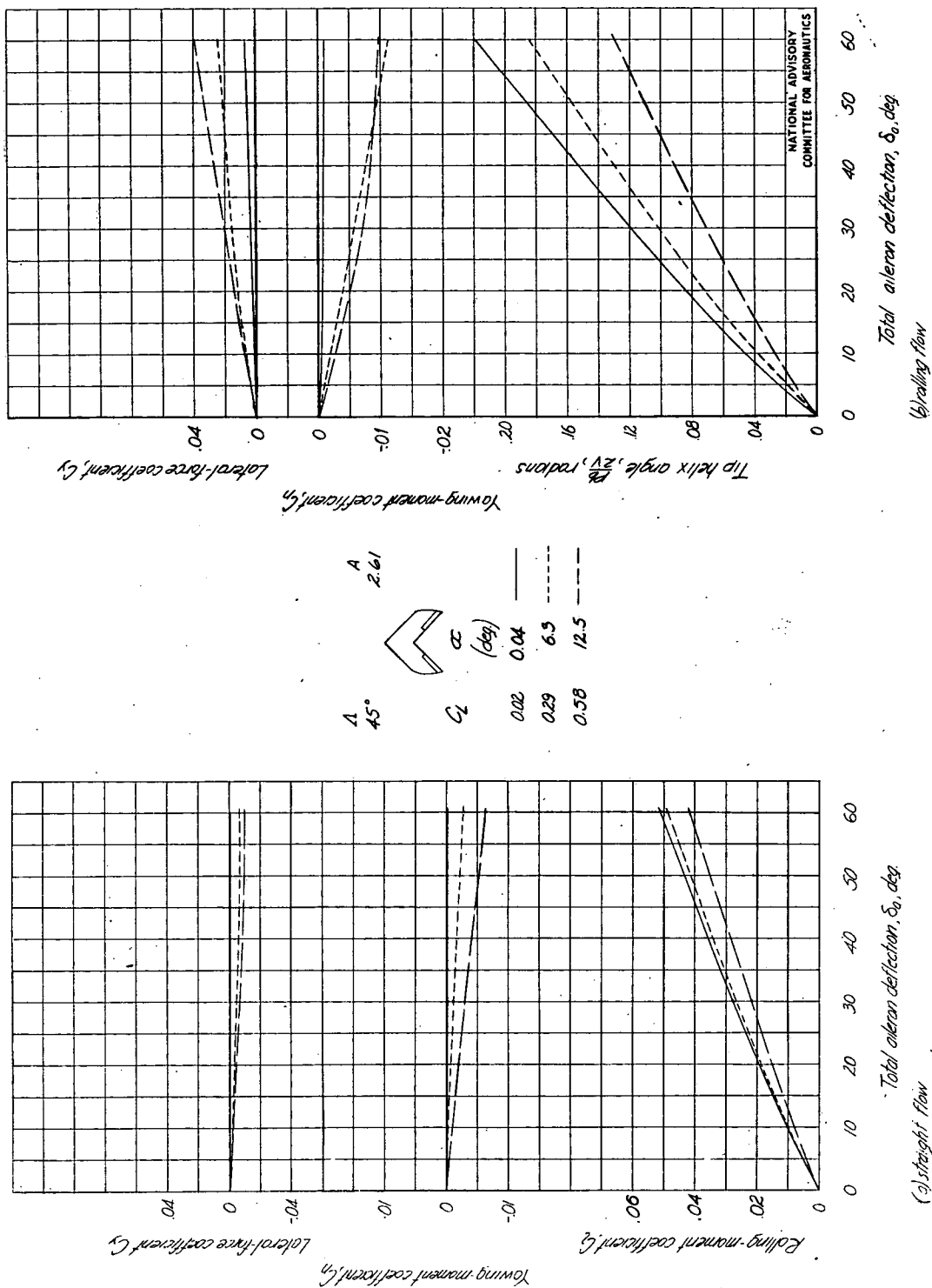


Figure 17.- Variation with aileron deflection of the aerodynamic characteristics of a rectangular 45° swept-back wing with 0.20 chord, 0.50 b/c.